https://doi.org/10.2352/AIT.2024.1.1.38

Decreasing measurement error for rub resistance of printouts located on previously bent substrates: development of device and method

Frédéric Mondiot, Claudiu Neagu, Serge Marchioni and Frédéric Bodino, Markem-Imaje, Marly, Switzerland.
Philip Kessler and Benoît Sahli, iPrint Institute, HEIA-FR, HES-SO University of Applied Sciences and Arts Western Switzerland, Fribourg, Switzerland.
Jan Huber and Gabrielle Thurnherr, iSIS Institute, HEIA-FR, HES-SO University of Applied Sciences and Arts Western Switzerland, Fribourg, Switzerland.

Abstract

Rub resistance is a parameter of major importance for the quality of inkjet printouts used in marking and coding. Yet, it becomes challenging to evaluate when the substrate has been bent prior to testing, like in the case of electrical cables, wires, or optical fibers.

This communication presents a solution embodied by a prototype machine specifically designed and built for this purpose and a testing method associated with it. In particular, all the parameters of interest, i.e. the bending speed, angle and radius, and the rubbing speed and applied force can be adjusted over a range representative of the real industrial constraints. The processing of the data allows for a precise quantification of the rub resistance of the ink printed on previously bent substrates.

Introduction

Methods widely used in the industry to evaluate rub resistance of inkjet printouts on electrical cables, wires, or optical fibers rely on bending the substrate supposedly around the finger and rubbing it with the thumb. Resistance of the printout to rubbing is assessed visually. Intrinsically, this approach to evaluate rub resistance comes with a high degree of variability.

The high variability of this method calls for a more structured and systematic approach to evaluating the rub resistance in this setting. The solution is an operator-independent, automated method.

I. The Cable Bending and Rubbing Machine: The main modules

The cable bending and rubbing machine is composed of three main modules: The cable bending and tensioning module, the rubbing module, and the imaging module (Figure 1). Moreover, the machine was developed around a central axis of revolution - the vertical axis **z** - located at the center of the bending wheel, that is part of the bending and tensioning module (Figure 2).

A. Cable bending and tensioning module

The cable is held in place by the bending wheel and the cable tensioning component (Figure 1b and Figure 2).

The former guides the cable. It has a small groove to support the cable and prevent it from moving vertically. The cable is further clamped in place by a plate with small grooves. It is tightened in place with the aid of a screw. Bending wheels of different sizes can be employed to change the cable bending radius and accommodate cables with diameters in the range of 3 to 20mm. Furthermore, the wheel is mounted on an axle, which is driven via a transmission by a stepper motor. This stepper motor, equipped with an encoder, allows the control of the wheel rotation

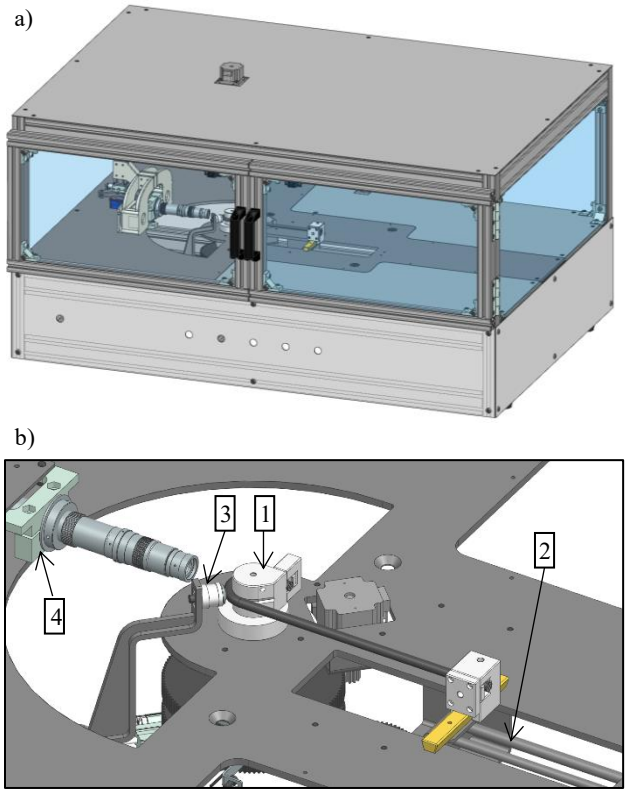

Figure 1. *a) Model view of the Cable Bending and Rubbing Machine. b) Model view of the main modules and components. The cable bending and tensioning module consists of (1) the bending wheel and (2) the tensioning component to which the cable in black is attached. (3) The abrading part of the rubbing module. (4) The camera (imaging module).*

and speed, and subsequent bending of the cable around the axis **z** in the angular range [0°, 220°] (Figure 2). The motor was positioned next to the axle to provide sufficient torque to bend large cables. A static capacitive sensor is used to detect the homing position of the axle.

Figure 3 shows the output angular bending speed as a function of the angular position of the bending wheel for input angular speeds of 90°/s (solid line) and 180 °/s (dashed line). Five measurements were carried out for each input angular speed. We note that all five curves overlap completely, and that each set value of the angular speed is precisely reached after an acceleration phase. This underlines the precision and repeatability of the bending process.

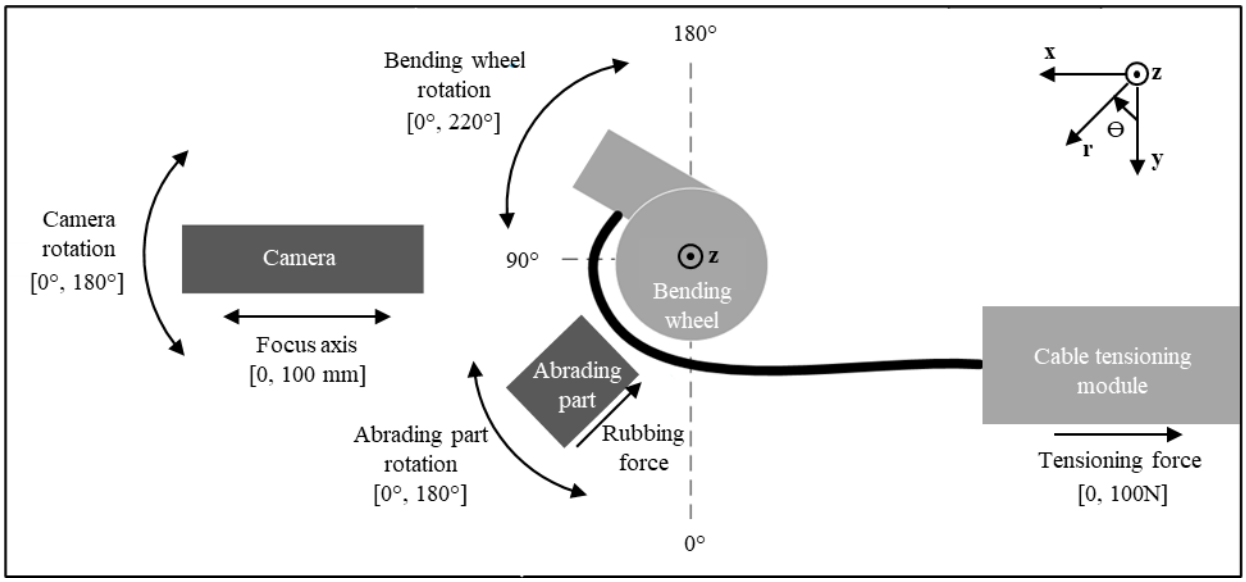

Figure 2. *Operating principle of the Cable Bending and Rubbing Machine.*

In addition, the tensioning component fastens the opposite end of the cable and ensures constant cable tension force by applying a precisely controlled air pressure via a cylinder. The position of the cable mounting can be moved orthogonally to the direction of tension to allow for different bending radii. The cable clamping mechanism is the same as the one placed on the bending wheels.

B. Rubbing module

The rubbing module consists of a silicone abrading part covered with a cotton fabric. This provides for a rubbing surface with a roughness comparable to that of the human thumb (Figure 4a). The vertical position of the abrading part can be manually aligned and centered on the cable surface. The abrading part is mounted on a pneumatic cylinder, equipped with a linear resistive sensor to read out the position of the piston. This allows for a tight control of the displacement of the abrading part both forward and backward, and the ensuing rubbing force applied to the cable along the radial axis **r** as depicted in Figure 2. The abrading part and its pneumatic cylinder are mounted on a stepper motor equipped with an encoder. This controls the angular position and speed of rotation around the common axis of revolution **z** within the angular range [0°,180°] (Figure 2).

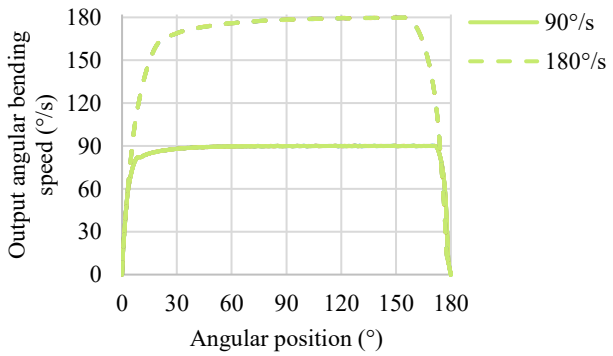

Figure 3. *Output angular bending speed vs. angular position of the bending wheel for two input angular speeds of 90°/s (solid line) and 180°/s (dashed line). For each input angular speed, five measurements were carried out, and all five curves overlapped.*

Figure 4b shows the output angular rubbing speed as a function of the angular position of the abrading part moving forward (positive values) and subsequently backward (negative values) for input angular speeds of 300, 350 and 400°/s. The bending angle was set to a value of 180° and the angular rubbing range to [30°, 150°]. All curves exhibit an acceleration phase, followed by a plateau at the exact input angular speed, and a deceleration phase. Therefore, the rubbing speed is controlled at high level of precision. The forward and reverse movements are very similar, with no noticeable deviation from the maximum velocity.

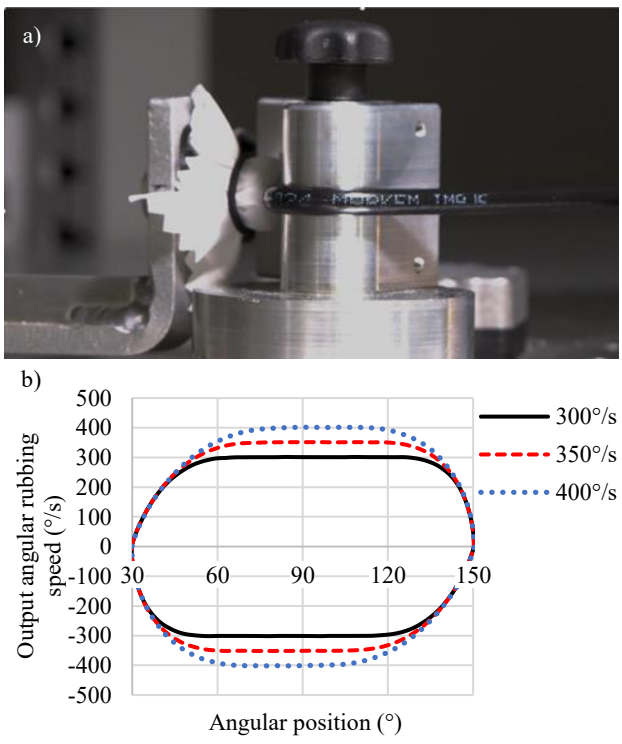

Figure 4. *a) Rubbing of a 5.4-mm-diameter cable bent to 180°. b) Output angular speed vs. angular position of the abrading part for input angular speeds of 300°/s (solid black line), 350°/s (dashed red line) and 400°/s (dotted blue line).*

C. Imaging module

The imaging module consists of a camera, two LEDs for illuminating the cable, and two moving axels. The first axel consists of a curved sliding bearing that is directly driven by a stepper motor equipped with an encoder and a gear reduction. This controls the angular position of the camera around the common axis of revolution **z** within the range [0°, 180°]. The second axle is mounted on the first one and consists of linear rolling guide bearings and a ball screw, which is driven by another stepper motor equipped with an encoder. This allows control of the radial position of the camera relative to the cable surface along **r**, which sets the plane of focus (Figure 2). With the minimum (respectively, maximum) zoom setting, the camera currently enables a field of view of 9.4 mm (respectively, 1.5 mm) and a resolution of 2.44 µm/px (respectively, 0.38 µm/px). The entire imaging module is mounted on silent blocks to reduce the transfer of vibrations from the machine to the camera.

II. Image processing

Image processing is the key element to provide sound statistical results and quantify the performance of the inks printed on the cable.

Image processing starts with a first image of the cable, before it is subjected to any rubbing process. The ink dots of the initial image are detected by a series of processing steps. The image is cropped to a user-specified Region of Interest (ROI). Then it undergoes several pre-processing steps before the dots are detected and analyzed.

A new picture is generated at the end of each rubbing cycle. These images are processed in the same manner and are corrected to be aligned with the initial image, compensating for cable displacement during the rubbing process.

Pre-processing starts with a blurring step. A Gaussian blur is applied to mitigate the impact of high-frequency artifacts that may negatively affect detection and analysis. A subtle blur balances noise reduction and maintains essential image details, enhancing the accuracy and reliability of subsequent analyses.

The second pre-processing step is thresholding. This is a technique used in image processing to segment an image into regions or objects based on pixel intensity. In simple terms, it involves setting a threshold value and classifying each pixel in the image as either foreground or background, depending on whether its intensity is above or below the threshold. After tests with different thresholding methods, Li's thresholding method was chosen due to its ability to produce superior and more distinct images.

The main detection is accomplished using OpenCV's "blob detection" method with specific parameter adjustments. Parameters such as brightness range, area of dots, and distance between dots are fine-tuned through a manual measurement process to optimize detection accuracy and reliability. The detection is then reapplied to the unprocessed image as a mask.

Data analysis can be finally carried out on a series of rubbed samples, and automatically processed to give statistics such as the average fraction and associated standard deviation of ink dots that have lost a given amount of relative brightness.

	Ink A	Ink B
Coefficient of Variation for manual method (CV_M) (%)	82	71
Coefficient of variation for automated method (CV_A) (%)	33	35
Relative coefficient of variation: (CV_M-CV_A) / CV_M (%)	60	51

Table 1. *Coefficients of variation for manual and automated methods as determined during a test session where the rub resistance of two inks A and B on previously bent cables was evaluated.*

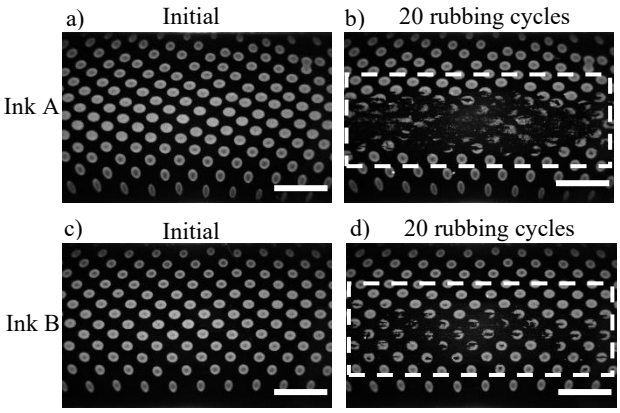

Figure 5. *Images at 90° of similar cables bent to 180° and printed with Ink A (a, b) and Ink B (c, d) before (a, c) and after (b, d) twenty back-and-forth rubbing cycles. The dashed white rectangles in b) and d) show the regions of interest for data processing. For Ink A (respectively, Ink B), 30% (respectively, 4%) of the dots have lost more than 80% of their initial brightness in a) (respectively, c). Scale bars: 2 mm.*

III. Current applications

A. Evaluation of ink rub resistance on previously bent cables

Industrial testing is essentially manual and the outcome depends on the operator. Typically, the cable is wrapped around the index finger of one hand, with no control over the bending force, and rubbed with the thumb of the other hand at the apex, i.e. at ~ 90° to the 180° bent cable. Rubbing speed and force are also subject to high variability.

Table 1 shows the high coefficients of variation associated with such a manual method during a test session with five different operators. During the session, they followed the manual bending process described previously and rubbed two cables each, printed with two different inks, A and B. Then they assessed the ink rub resistance by assigning grades according to the number of back-and-forth rubbing cycles required to remove the ink. The maximum number of back-and-forth rubbing cycles allowed was set to 20 (grade of 5). Ink A was removed below 5 back-and-forth rubbing cycles (grade of 1) for three operators, between 10 and 15 (grade of 3) for another one, while the last operator did not remove anything up to 20. The average grade for Ink A was hence 2.2 ± 1.8, so a derived coefficient of variation CV_M of 82% (Table 1). For Ink B, two operators gave a grade of 1, and the three other operators a grade of 2 (ink removed between 5 and 10 back-and-forth rubbing cycles), 3 and 5, respectively. The average grade for Ink B then was 2.4 ± 1.7, with an associated coefficient of variation CV_M of 71% (Table 1). Consequently, the manual method makes it difficult to distinguish between the performance of both inks, mainly due to the lack of control and repeatability of the bending and rubbing processes between the different operators.

In contrast, the prototype machine developed enables fine, reproducible control of bending radius, angle and speed, as well

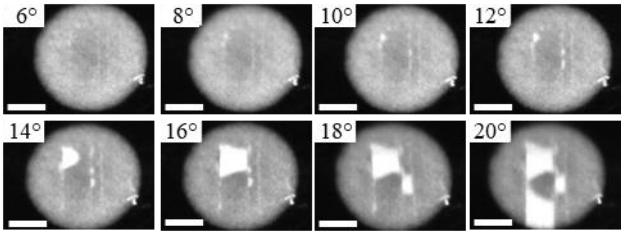

Figure 6. *Snapshots of a printed ink dot taken at different cable bending angles. Scale bars: 150 µm.*

as rubbing speed and applied force. As with the manual method, two series of five cables printed with Inks A and B were bent to 180°, with a bending radius of 1cm, close to the radius of curvature of the cable wrapped around the index finger. The bending speed was set to 90°/s. This mimics the operators' speed for wrapping the cable around the finger. The rubbing speed was set to 340°/s in the angular rubbing range [30°, 150°], which was found to reproduce the conditions of manual testing. The rubbing force was set to 3N, a typical value of the force a human thumb applies on the cable sheath while rubbing onto the printout. The abrading part was covered with a piece of cotton fabric, ISO Crock cloth as per ISO 105-F09, to provide with a rubbing surface with a roughness comparable to that of the human thumb. The piece of cloth was replaced with a fresh one after each sample had been tested. The camera was positioned at 90° to image and analyze the cable apex.

Figure 5 presents the results obtained for Inks A and B after twenty back-and-forth rubbing cycles. Data analysis shows that 30.0 ± 10.0% of the dots for Ink A and 4.0 ± 1.4% of the dots for Ink B lost 80% of their initial brightness. This results in coefficients of variation of 33% and 35% for Inks A and B, respectively (Table 1). In contrast to the manual, operator-dependent method, the automated method enables the two inks to be ranked unambiguously. Most importantly, it significantly decreases the values of the coefficients of variation due to the tight control and repeatability of the bending and rubbing processes. The prototype machine, combined with data processing software, offers a coefficient of variation gain of at least 50% over the manual one (Table 1).

B. Observation of dot alteration during the bending process

The automated cable bending process, combined with the imaging system, makes it possible to track the evolution of ink dot alteration as the cable is bent at different angles at a given bending speed and radius. As depicted in Figure 6, the continuous stretching of an ink dot along the horizontal axis as the cable is increasingly bent, leads to the formation and expansion of cracks within the printed dot. This can be used to determine a critical angular bending range ([6°, 8°] here) at which cracks are generated.

Conclusion and perspectives

A prototype machine allowing for an operator-independent automated method was developed. The settings, i.e. the bending radius and speed, cable tensioning force, rubbing speed and applied force can be controlled at a high level of precision and accuracy. As a result, the coefficient of variation of the test results decreased by at least 50% with respect to the operator-dependent manual method. The prototype machine also allows for expanded analysis regarding the behavior of the printout such as presence of cracks.

This is the first highly automated and controlled solution in the industry. This solution is expected to replace the widely used, unstandardized, and high variability operator-dependent approach.

Author Biography

Frédéric Mondiot, PhD in Physical Chemistry of Condensed Matter from the University of Bordeaux, France, has over 10 years' experience in research and development in the field of cutting-edge composite materials. Currently at Markem-Imaje, he is performing research and developing inks for digital printing.

Claudiu Neagu, PhD in Physical Chemistry of Polymers from Queen's University at Kingston with over 25 years of international experience in providing innovative and disruptive solutions through research, development and quality assurance. Currently, Global Analytical Chemistry Manager with Markem-Imaje, Switzerland.